Bulletin of the JSME Vol.8, No.3, 2021
Mechanical Engineering Journal

Optimal design of a series-type double-mass hysteretically damped dynamic vibration absorber based on the stability criterion

Toshihiko ASAMI* and Keisuke YAMADA**
* Department of Mechanical Engineering, University of Hyogo
2167 Shosha, Himeji, Hyogo 671-2280, Japan
E-mail: asami@eng.u-hyogo.ac.jp
** Department of Mechanical Engineering, Kansai University
3-3-35 Yamate-cho, Suita, Osaka 564-8680, Japan

Received: 11 November 2020; Revised: 25 March 2021; Accepted: 1 June 2021

Abstract
In most dynamic vibration absorbers (DVAs) used in practical applications, polymeric materials that have both restoring capabilities and damping effects are used instead of coil springs as spring elements. It is known that the damping force for such polymeric materials has hysteretic characteristics and varies in proportion to the relative displacement rather than the relative velocity between objects. This paper proposes an optimal design formula for a double-mass hysteretically damped DVA with two masses connected in series. For the design of the DVA in this study, the stability maximization criterion, which attenuates the free-vibration response of the primary system in the shortest time, was adopted. It was found that the optimal design expression for installing the series-type double-mass DVA on an undamped primary system can be expressed by a very simple formula. The maximized stability, which determines the speed of vibration convergence, of the double-mass DVA was 1.7 times that of the corresponding single-mass DVA. When there is damping in the primary system, the optimal design condition for the DVA cannot be expressed with such a simple formula, but an equation to calculate it is presented in this paper. The equation can be easily solved numerically, and the results show that the stability of the system is further increased compared to the undamped primary system.

Keywords : Vibration, Optimal design, Transient vibration, Hysteretically damped dynamic vibration absorber, Series-type double-mass absorber, Stability maximization criterion, Damped primary system

1. Introduction

The dynamic vibration absorber (DVA), which is a small vibration suppression device, is said to have been first devised to reduce the rolling vibrations of ships (Watts, 1883). Since then, several criteria have been proposed for the optimal design of DVAs, which are now used in various structures such as buildings, railroad vehicles, automobiles, and vibration isolators. Typical design criteria for DVA proposed so far include the H_∞ optimization criterion for minimizing the height of the resonant point of a system in steady-state vibration under periodic excitation (Ormondroyd and Den Hartog, 1928), the H_2 optimization criterion for minimizing the total kinetic energy over the entire frequency range rather than just at the resonant point (Crandall and Mark, 1963), and the stability maximization criterion for minimizing the convergence time of the free-vibration response instead of the steady-state response (Nishihara and Matsuhisa, 1997).

Recently, to improve the performance and robustness of DVAs, multi-mass DVAs, in which two or more DVA masses are combined, have been studied (Iwanami and Seto, 1984; Yasuda and Pan, 2003). The present authors have also worked on the optimization of the double-mass DVA and have confirmed that its performance is significantly better than that of the single-mass DVA, especially when the two masses are connected in series (Asami, 2019; Asami and Yamada, 2020). The results of these DVA optimization studies were obtained under the assumption that the vibratory system is viscously damped. The analytical model is shown in Fig. 1(b).

Paper No.20-00476
J-STAGE Advance Publication date : 10 June, 2021
[DOI: 10.1299/mej.20-00476]

Most DVAs in practical use do not consist of a coil spring, dashpot, and mass, as shown in Fig. 1(b), but are manufactured by combining masses with polymer materials that have both restoring capabilities and damping effects. Experimentally, the damping force for this polymer material is known to vary roughly in proportion to the relative displacement between objects rather than their relative velocity (Shibata et al., 1993). This type of damping force is called hysteretic damping and is often modeled mathematically as shown in Fig. 1(a). Note that even in viscously damped systems, the load-displacement curve follows a hysteresis loop, but the shape of this loop is affected by the frequency, whereas in hysteretically damped systems it is not affected by the frequency (Asami et al., 2020). In many cases, the damping of the primary system is the result of internal damping within the materials that make up the primary system and of structural damping due to the friction of the contacting parts. These attenuation characteristics are also better modeled with hysteretic damping than with viscous damping.

There have been few studies on the optimization of the hysteretically damped DVA shown in Fig. 1(a), and the present authors previously studied the case of hysteretic damping in a single-mass DVA (Asami et al., 2020). This work is a continuation of that study and proposes an optimal design formula for a series-type double-mass hysteretically damped DVA. In the previous study, the optimal solution was derived for all three DVA design criteria described above, but in the present study, the DVA was optimized only for the stability maximization criterion because the other two criteria could not be algebraically solved.

As in the case of the viscously damped DVA, the performance of the hysteretically damped DVA is significantly improved with the use of a series-type double-mass DVA instead of a single-mass DVA. The stability of the double-mass DVA was found to be approximately 1.7 times that of the single-mass DVA with respect to the typical mass ratio of the DVA to the primary system. Moreover, when there is no damping in the primary system, the formula that gives the optimal design values for the DVA is very simple. In contrast, when the primary system has damping, the optimal DVA design conditions cannot be obtained without solving a higher-order algebraic equation. In this paper, the equation and the optimal design values for the DVA obtained by solving it numerically are presented. From these solutions, it is shown that the stability can be further increased when damping is present in the primary system. Finally, the free-vibration responses of a primary system and two DVAs connected in series are presented and their vibration suppression effect is visualized.

2. Analytical model and definition of dimensionless parameters

Figure 1(a) shows the hysteretically damped three-degree-of-freedom (3-DOF) system considered in this study. In this figure, P is the primary system to be suppressed, and DVA-A and DVA-B are two vibration absorbers connected in series. The springs connecting the three masses have hysteretic damping characteristics, which are expressed by the loss factors η_i, $(i = 1\text{–}3)$. Figure 1(b) shows a 3-DOF viscously damped system, which is assessed for comparison with the hysteretically damped system. The optimal values of the DVA for reducing the free-vibration response of these vibratory systems and the differences in the free and steady-state responses of the systems are discussed in this paper.

The response of the system can be fully expressed by the following dimensionless parameters:

$$\mu = \frac{m_2 + m_3}{m_1},\ \mu_B = \frac{m_3}{m_2},\ \nu = \frac{\omega_2}{\omega_1},\ \nu_B = \frac{\omega_3}{\omega_2},\ \lambda = \frac{\omega}{\omega_1},\ \tau = \omega_1 t,\ \zeta_1 = \frac{c_1}{2m_1\omega_1},\ \zeta_2 = \frac{c_2}{2m_2\omega_2},\ \zeta_3 = \frac{c_3}{2m_3\omega_3}, \quad (1)$$

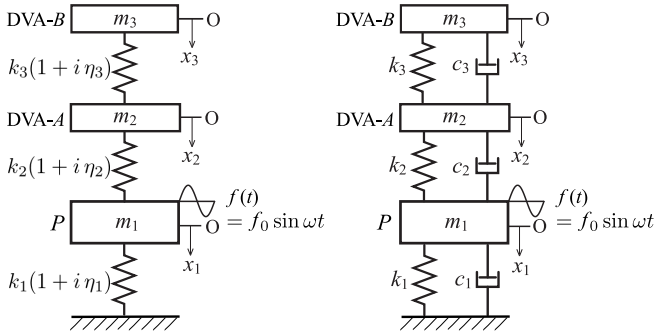

(a) Hysteretically damped 3-DOF system (b) Viscously damped 3-DOF system

Fig. 1 Analytical models of 3-DOF vibratory systems. Representation of hysteretically damped systems using the imaginary unit i is a convenient method of calculating the steady-state response for systems subjected to periodic external forces, but a serious contradiction arises in the calculation of the free-vibration response to initial disturbances.

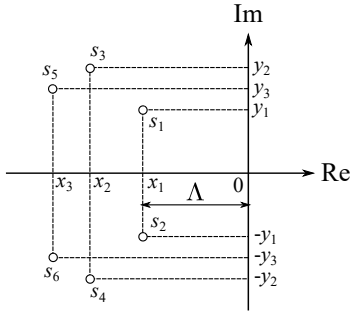

Fig. 2 Characteristic roots of a viscously damped 3-DOF system. The real part of the characteristic roots represents the speed of vibration decay, and the imaginary part represents the damped natural angular frequency. The stability Λ describes how quickly the free vibration decays.

[DOI: 10.1299/mej.20-00476]

where ω_1, ω_2 and ω_3 are the undamped angular natural frequencies of each vibratory system and are defined as

$$\omega_1 = \sqrt{k_1/m_1},\ \ \omega_2 = \sqrt{k_2/m_2},\ \ \omega_3 = \sqrt{k_3/m_3}. \tag{2}$$

3. Stability maximization criterion

In this study, the stability maximization criterion for the design of a DVA was adopted. In this approach, the free-vibration response of the primary system is made to converge in the shortest possible time (for this purpose, the periodic excitation force shown in Fig. 1 is replaced by an impulse input). Figure 2 shows the characteristic roots of a viscously damped 3-DOF system plotted in the complex plane. The imaginary part of the characteristic root represents the damped natural angular frequency, indicating that the system has three natural frequencies. The real part of the characteristic root, which is negative in a stable system, indicates the speed of convergence of each natural vibration. The rightmost characteristic root (s_1 and s_2 in this figure) determines the speed of convergence of the free vibration. The horizontal distance between the rightmost characteristic root and the imaginary axis is called the stability of the system, which is defined as (Nishihara and Matsuhisa, 1997)

$$\Lambda = -\max(\mathrm{Re}[s_i]). \tag{3}$$

Maximizing the value of Λ is the goal of DVA design by the stability maximization criterion.

As described in our previous paper (Asami, et al., 2020), in the hysteretically damped system shown in Fig. 1(a), the complex conjugate roots shown in Fig. 2 do not appear. Instead, a second characteristic root appears at a point-symmetric position about the coordinate origin from the first characteristic root appearing in the second quadrant in the complex plane. Since the real part of this characteristic root is positive, the vibratory system is inevitably unstable. This happens because the properties of the hysterically damped system are expressed using the imaginary unit i (resulting in a positive phase shift in the output relative to the input). Such a representation is not problematic when applied to the calculation of the steady-state response (forced-vibration response) if a periodic input is applied to the system. However, a serious discrepancy arises when calculating the free vibration after an impulse is input to the system. In this study, the stable free vibration response was calculated by a method proposed by one of the authors (Yamada, 2020), i.e., by the superposition of the forced vibration response.

4. Design of hysteretically damped double-mass vibration absorbers based on stability criterion

4.1. Derivation of characteristic equations using triple roots

The characteristic equation for the vibratory system shown in Fig. 1(a) is

$$(1+\mu_B)S^6 + (a_1 + i\,b_1)S^4 + (a_2 + i\,b_2)S^2 + (a_3 + i\,b_3) = 0. \tag{4}$$

The characteristic root s shown in Fig. 2 has units of angular frequency, whereas the parameter S $(= s/\omega_1)$ shown here represents the dimensionless characteristic root. The parameters used in Eq. (4) are given as follows with respect to the dimensionless parameters defined in Eq. (1):

$$\left.\begin{aligned}
a_1 &= (1+\mu_B)(1+\nu^2) + \mu\nu^2 + (1+\mu_B)^2\nu^2\nu_B^2 \\
b_1 &= \eta_1(1+\mu_B) + \eta_2(1+\mu+\mu_B)\nu^2 + \eta_3(1+\mu_B)^2\nu^2\nu_B^2 \\
a_2 &= (1+\mu_B)\nu^2\{1 + [1+\mu_B + (1-\eta_2\eta_3)(1+\mu)\nu^2]\nu_B^2 - \eta_1[\eta_2 + \eta_3(1+\mu_B)\nu_B^2]\} \\
b_2 &= (1+\mu_B)\nu^2\{\eta_1[1+(1+\mu_B)\nu_B^2] + \eta_2[1+(1+\mu)\nu^2\nu_B^2] + \eta_3[1+\mu_B+(1+\mu)\nu^2]\nu_B^2\} \\
a_3 &= (1-\eta_1\eta_2-\eta_2\eta_3-\eta_3\eta_1)(1+\mu_B)\nu^4\nu_B^2 \\
b_3 &= (\eta_1+\eta_2+\eta_3-\eta_1\eta_2\eta_3)(1+\mu_B)\nu^4\nu_B^2.
\end{aligned}\right\} \tag{5}$$

In studies on the optimization of series-type double-mass DVAs for viscously damped systems (Asami, 2017; Asami et al., 2018), it has been found that the damping ratio ζ_2 for DVA-A (Fig. 1(b)) should be smaller. Therefore, zero is the optimal value because a negative damping ratio cannot be achieved with non-active elements. Furthermore, it is known that the real parts of the characteristic roots are in a trade-off relationship and must be equal to maximize the system stability Λ (Asami et al., 2018). The imaginary parts of the characteristic roots are then equal as well. In other words, the stability is maximized when the system has a triple root. If the coordinate of this triplet is denoted as $\sqrt{a_0 + i\,b_0}$, Eq. (4) can then be expressed as

$$(1+\mu_B)(S - \sqrt{a_0 + i\,b_0})^3(S + \sqrt{a_0 + i\,b_0})^3 = 0. \tag{6}$$

[DOI: 10.1299/mej.20-00476]

Expanding Eq. (6) and equating the real and imaginary parts with Eq. (4), we can derive the following system of six simultaneous algebraic equations:

$$\left.\begin{aligned}
f_1 &= (1+3a_0)(1+\mu_B) + (1+\mu+\mu_B)\nu^2 + (1+\mu_B)^2\nu^2\nu_B^2 = 0\\
f_2 &= 3b_0 + \eta_1 + \eta_3(1+\mu_B)\nu^2\nu_B^2 = 0\\
f_3 &= -3(a_0^2 - b_0^2) + \nu^2 + (1+\mu)\nu^4\nu_B^2 + (1+\mu_B)(1-\eta_1\eta_3)\nu^2\nu_B^2 = 0\\
f_4 &= -6a_0b_0 + \eta_1\nu^2 + \eta_1(1+\mu_B)\nu^2\nu_B^2 + \eta_3[1+\mu_B+(1+\mu)\nu^2)]\nu^2\nu_B^2 = 0\\
f_5 &= a_0(a_0^2 - 3b_0^2) + (1-\eta_1\eta_3)\nu^4\nu_b^2 = 0\\
f_6 &= b_0(3a_0^2 - b_0^2) + (\eta_1+\eta_3)\nu^4\nu_b^2 = 0,
\end{aligned}\right\} \tag{7}$$

where η_2 was set to zero. Equation (7) is a set of simultaneous equations with six unknowns ($\mu_B, \nu, \nu_B, \eta_3, a_0, b_0$) because μ and η_1 are given. Therefore, the solution can be obtained by ordinary algebraic manipulation.

4.2. Derivation of the optimal solution for an undamped primary system

As a special case, if there is no damping in the primary system, i.e., $\eta_1 = 0$, the solution to Eq. (7) is obtained as follows:

$$\left.\begin{aligned}
&\mu_B = \frac{8\mu(1+\mu)}{(1-\mu)^2}, \quad \nu = \frac{1+3\mu}{(1+\mu)\sqrt{1-\mu}}, \quad \nu_B = \frac{(1-\mu)\sqrt{(1+\mu)(1-9\mu)}}{(1+3\mu)^2}, \quad \eta_3 = \frac{3(1-\mu)\sqrt{3\mu}}{1-9\mu}\\
&a_0 = -\frac{1}{1+\mu}, \quad b_0 = -\frac{\sqrt{3\mu}}{1+\mu}.
\end{aligned}\right\} \tag{8}$$

This solution is confirmed to be the only real root of Eq. (7). If the coordinates of the dimensionless characteristic roots are denoted as $S_1(x_1, y_1)$ and $S_2(x_2, y_2)$, then by the method presented in our previous paper (Asami, et al., 2020), these coordinates can be calculated using a_0 and b_0 in Eq. (8) as follows:

$$x_1 = -\sqrt{\frac{-1+\sqrt{1+3\mu}}{2(1+\mu)}}, \quad y_1 = i\sqrt{\frac{1+\sqrt{1+3\mu}}{2(1+\mu)}} \tag{9}$$

and

$$x_2 = \sqrt{\frac{-1+\sqrt{1+3\mu}}{2(1+\mu)}}, \quad y_2 = -i\sqrt{\frac{1+\sqrt{1+3\mu}}{2(1+\mu)}}. \tag{10}$$

The characteristic roots in the viscously damped system appear as complex conjugates, as shown in Fig. 2, whereas in the hysteretically damped system, the two complex roots $S_1(x_1, y_1)$ and $S_2(x_2, y_2)$ are point-symmetric about the coordinate origin. Among these two roots, the root S_2 is unstable. Therefore, the free-vibration response of the hysteretically damped system cannot be calculated using the usual method. Because what appears in the forced vibration is the characteristic root S_1, if we collectively display the solution of the stability criterion of DVA for an undamped primary system, noting that $\Lambda = -x_1$, we find that

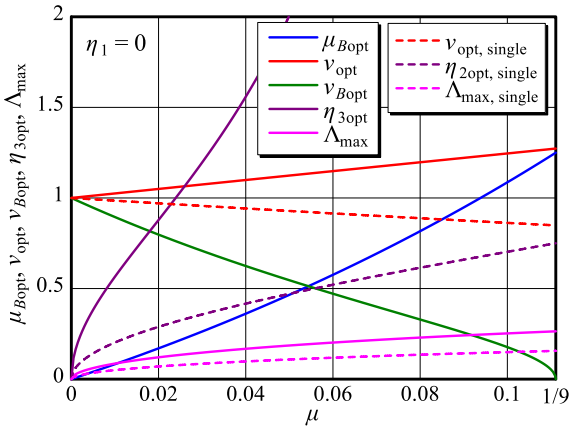

Fig. 3 Optimal solution for a series-type double-mass hysteretically damped DVA in an undamped primary system based on the stability criterion. The region in which the characteristic equations can take a triple root is limited to $\mu < 1/9$. The solid pink line shows the maximized stability of the system with the double-mass DVA, $\Lambda_{\max}$. This stability is 1.7 times higher than that of the system with a single-mass DVA (dashed pink line).

[DOI: 10.1299/mej.20-00476]

$$\left.\begin{aligned} &\mu_{B\mathrm{opt}} = \frac{8\mu(1+\mu)}{(1-\mu)^2}, \quad \nu_{\mathrm{opt}} = \frac{1+3\mu}{(1+\mu)\sqrt{1-\mu}}, \quad \nu_{B\mathrm{opt}} = \frac{(1-\mu)\sqrt{(1+\mu)(1-9\mu)}}{(1+3\mu)^2} \\ &\eta_{2\mathrm{opt}} = 0, \quad \eta_{3\mathrm{opt}} = \frac{3(1-\mu)\sqrt{3\mu}}{1-9\mu}, \quad \Lambda_{\max} = \sqrt{\frac{-1+\sqrt{1+3\mu}}{2(1+\mu)}}. \end{aligned}\right\} \tag{11}$$

For comparison, the solution based on the stability criterion for a hysteretically damped single-mass DVA in an undamped primary system is as follows (Asami, et al., 2020):

$$\nu_{\mathrm{opt,\ single}} = \frac{\sqrt{1-\mu}}{1+\mu}, \quad \eta_{2\mathrm{opt,\ single}} = \frac{2\sqrt{\mu}}{1-\mu}, \quad \Lambda_{\max,\mathrm{single}} = \sqrt{\frac{1}{2}\left(\sqrt{\frac{1}{1+\mu}} - \frac{1}{1+\mu}\right)}. \tag{12}$$

Equations (11) and (12) are plotted against the mass ratio μ of the DVA to the primary system in Fig. 3 with solid and dashed lines, respectively. For a hysteretically damped double-mass DVA system, the region in which the characteristic equation takes a triple root is restricted to the narrow range of $\mu < 1/9$. In contrast, it is clear from Eq. (12) that the region in which the system with a hysteretically damped single-mass DVA takes a double root has $\mu < 1$. The optimal solution for the DVA based on the stability criterion should exist for all values of μ, but the derivation of the solution in the region beyond the range of this figure is a subject for future work. As shown in Fig. 3, it is noteworthy that the stability of the system with a double-mass DVA is much higher (approximately 1.7 times) than that of the system with a single-mass DVA in the case of hysteretically damped systems. The effect of this increase in stability on the free-vibration response of the system will be explained in Section 4.6.

4.3. Derivation of the optimal solution for a damped system

In the case of a damped primary system, the optimal solution cannot be expressed by a simple equation like Eq. (11). The simplest equation available at the moment is presented below.

First, the last parameter b_0 in Eq. (8) was computed as a root of the following higher-order equation:

$$\left.\begin{aligned} f_b &= d_0 b_0^{12} + d_1 b_0^{11} + d_2 b_0^{10} + d_3 b_0^9 + d_4 b_0^8 + d_5 b_0^7 + d_6 b_0^6 + d_7 b_0^5 + d_8 b_0^4 + d_9 b_0^3 + d_{10} b_0^2 + d_{11} b_0 + d_{12} = 0 \\ d_0 &= 432(1+\mu)^6 \\ d_1 &= 864\,\eta_1(1+\mu)^5(5+\mu) \\ d_2 &= -144(1+\mu)^4[\,9\mu - \eta_1^2(136+67\mu+4\mu^2)] \\ d_3 &= -16\,\eta_1(1+\mu)^3[\,27\mu(23+7\mu) - \eta_1^2(3322+2895\mu+525\mu^2+8\mu^3)] \\ d_4 &= -72\,\eta_1^2(1+\mu)^2[\,\mu(467+374\mu+35\mu^2) - \eta_1^2(1334+1775\mu+620\mu^2+51\mu^3)] \\ d_5 &= -288\,\eta_1^3(1+\mu)^2[\,\mu(229+104\mu+3\mu^2) - \eta_1^2(422+365\mu+74\mu^2+3\mu^3)] \\ d_6 &= -24\,\eta_1^2[\,9\mu^2(1-6\mu+\mu^2) + 2\eta_1^2\mu(4+\mu)(431+856\mu+403\mu^2+2\mu^3) \\ &\quad - \eta_1^4(4592+11344\mu+9131\mu^2+2674\mu^3+227\mu^4+4\mu^5)] \\ d_7 &= -72\,\eta_1^3[\,\mu^2(13-54\mu+5\mu^2) + 2\eta_1^2\mu(480+1021\mu+522\mu^2+53\mu^3) \\ &\quad - \eta_1^4(1000+2144\mu+1283\mu^2+214\mu^3+3\mu^4)] \\ d_8 &= -9\,\eta_1^4[\,\mu^2(181-518\mu+21\mu^2) + 2\eta_1^2\mu(2152+4557\mu+1778\mu^2+93\mu^3) \\ &\quad - \eta_1^4(3728+7024\mu+2683\mu^2+86\mu^3-21\mu^4)] \\ d_9 &= -6\,\eta_1^5[\,\mu^2(241-474\mu+5\mu^2) + 2\eta_1^2\mu(1192+2633\mu+734\mu^2+13\mu^3) \\ &\quad - \eta_1^4(1808+3056\mu+447\mu^2-86\mu^3-5\mu^4)] \\ d_{10} &= -9\,\eta_1^4[\,\mu^3 + \eta_1^2\mu^2(76-101\mu) + \eta_1^4\mu(368+888\mu+163\mu^2) - \eta_1^6(256+400\mu-44\mu^2-9\mu^3)] \\ d_{11} &= -9\,\eta_1^5[\,\mu^3 + 3\eta_1^2\mu^2(6-5\mu) + 3\eta_1^4\mu(16+44\mu+5\mu^2) - \eta_1^6(32+48\mu-18\mu^2+\mu^3)] \\ d_{12} &= -\eta_1^6[\,2\mu^3 + 3\eta_1^2\mu^2(5-2\mu) + 6\eta_1^4\mu(4+13\mu+\mu^2) - \eta_1^6(4-\mu)^2(1+2\mu)]. \end{aligned}\right\} \tag{13}$$

Although there are 12 solutions to Eq. (13) including complex roots, it was found that the optimal solution is the negative minimum real root. Substituting one of the solutions obtained in this way into the following equation yields the other solutions of Eq. (7):

$$\left.\begin{aligned} a_0 &= -\frac{3b_0^2(1+\mu) + b_0\eta_1(4+3\mu) + \eta_1^2(1+\mu)}{3b_0^2(1+\mu)^2 + 2b_0\eta_1(1+\mu)(2+\mu) + \eta_1^2(1+2\mu)} \\ \mu_{B\mathrm{opt}} &= \mu_{BN}/\mu_{BD} \\ \nu_{\mathrm{opt}} &= \sqrt{\nu_{2N}/\nu_{2D}} \\ \nu_{B\mathrm{opt}} &= \sqrt{\nu_{B2N}}/\nu_{BD} \\ \eta_{3\mathrm{opt}} &= \eta_{3N}/\eta_{3D}, \end{aligned}\right\} \tag{14}$$

[DOI: 10.1299/mej.20-00476]

where

$$
\left.
\begin{aligned}
\mu_{BN} &= 27b_0^4(1+\mu)^2 + 9b_0^3\eta_1(1+\mu)(5+7\mu) - 3b_0^2[3(1+\mu) - \eta_1^2(10+28\mu+19\mu^2) + 6a_0(1+\mu) \\
&\quad + 3a_0^2(1+\mu)^2] - 3b_0\eta_1\{(3+4\mu)[1-\eta_1^2(1+2\mu)] + 2a_0(3+4\mu) + 3a_0^2(1+\mu)^2\} \\
&\quad - \eta_1^2[3+4\mu-\eta_1^2(1+2\mu)^2 + 6a_0(1+\mu) + 3a_0^2(1+\mu+\mu^2)] \\
\mu_{BD} &= [3(1+2a_0)b_0 + (2+3a_0)\eta_1]^2(1+\mu) \\
\nu_{2N} &= -27b_0^4(1+\mu)^2 - 9b_0^3\eta_1(1+\mu)(5+7\mu) - 3b_0^2\eta_1^2(10+28\mu+19\mu^2) \\
&\quad - 3b_0\eta_1[1+\eta_1^2(1+2\mu)(3+4\mu)] - \eta_1^2[1+\eta_1^2(1+2\mu)^2] \\
&\quad - 6a_0[\eta_1^2(1+\mu) + b_0\eta_1(4+3\mu) + 3b_0^2(1+\mu)] - 3a_0^2[\eta_1^2(2+2\mu-\mu^2) + 3b_0(b_0+\eta_1)(1+\mu)(3-\mu)] \\
\nu_{2D} &= [3(1+2a_0)b_0 + (2+3a_0)\eta_1](1+\mu)[\eta_1(1+2\mu) + 3b_0(1+\mu)] \\
\nu_{B2N} &= [3(1+2a_0)b_0 + (2+3a_0)\eta_1]^2(1+\mu)[\eta_1(1+2\mu) + 3b_0(1+\mu)]\{-9b_0^3(1+\mu) - 3b_0^2\eta_1(4+5\mu) \\
&\quad + 3b_0[1-\eta_1^2(2+3\mu) + a_0(3+\mu) + 3a_0^2(1+\mu)] + \eta_1[1-\eta_1^2(1+2\mu) + 3a_0(1+\mu) + 3a_0^2(1+2\mu)]\} \\
\nu_{BD} &= 27b_0^4(1+\mu)^2 + 9b_0^3\eta_1(1+\mu)(5+7\mu) + 3b_0^2\eta_1^2(10+28\mu+19\mu^2) \\
&\quad + 6a_0[3b_0^2(1+\mu) + b_0\eta_1(4+3\mu) + \eta_1^2(1+\mu)] + \eta_1^2[1+\eta_1^2(1+2\mu)^2] \\
&\quad + 3a_0^2[3b_0(b_0+\eta_1)(1+\mu)(3-\mu) + \eta_1^2(2+2\mu-\mu^2)] + 3b_0\eta_1[1+\eta_1^2(1+2\mu)(3+4\mu)] \\
\eta_{3N} &= -(3b_0+\eta_1)[3(1+2a_0)b_0 + (2+3a_0)\eta_1](1+\mu) \\
\eta_{3D} &= 9b_0^3(1+\mu) + 3b_0^2\eta_1(4+5\mu) - 3b_0[1-\eta_1^2(2+3\mu) + a_0(3+\mu) + 3a_0^2(1+\mu)] \\
&\quad - \eta_1[1-\eta_1^2(1+2\mu) + 3a_0(1+\mu) + 3a_0^2(1+2\mu)].
\end{aligned}
\right\} \quad (15)
$$

Furthermore, the coordinates of the characteristic triple roots can be calculated as

$$
x_1 = -\sqrt{\frac{1}{2}\left(a_0 + \sqrt{a_0^2+b_0^2}\right)}, \quad y_1 = i\sqrt{\frac{1}{2}\left(-a_0 + \sqrt{a_0^2+b_0^2}\right)}. \quad (16)
$$

4.4. Trajectories of the characteristic root when the solution takes a multiple root

Figure 4(a) shows a plot of the coordinates $S_1(x_1, y_1)$ of the triple characteristic root calculated by Eq. (16), and Fig. 4(b) shows the coordinates for a system with a hysteretically damped single-mass DVA when the characteristic equation takes a double root (Asami et al., 2020). In this case, we show the trajectory of the double roots in the range of $0 \le \mu \le 1$ and $0 \le \eta_1 \le 1.2$. It should be noted that the scales of the coordinate axes in Fig.4 (a) and (b) are different because the region in which the characteristic equation can take a triple root is limited to a very small range of μ and η_1. These characteristic roots exist in the second quadrant of the complex plane. In the hysteresis decay system modeled as in Fig. 1(a), another characteristic root $S_2(x_2, y_2)$ exists in the fourth quadrant, taking the form of the Fig. 4 rotated 180° about the coordinate origin (0, 0).

One of the characteristics of the hysteretically damped system is that the damped natural frequencies are larger than the undamped ones. This can be understood from the fact that the curve of constant μ rises to the left, which is the opposite of what happens in the viscously damped system. In contrast, the curve for constant η_1 falls to the left in

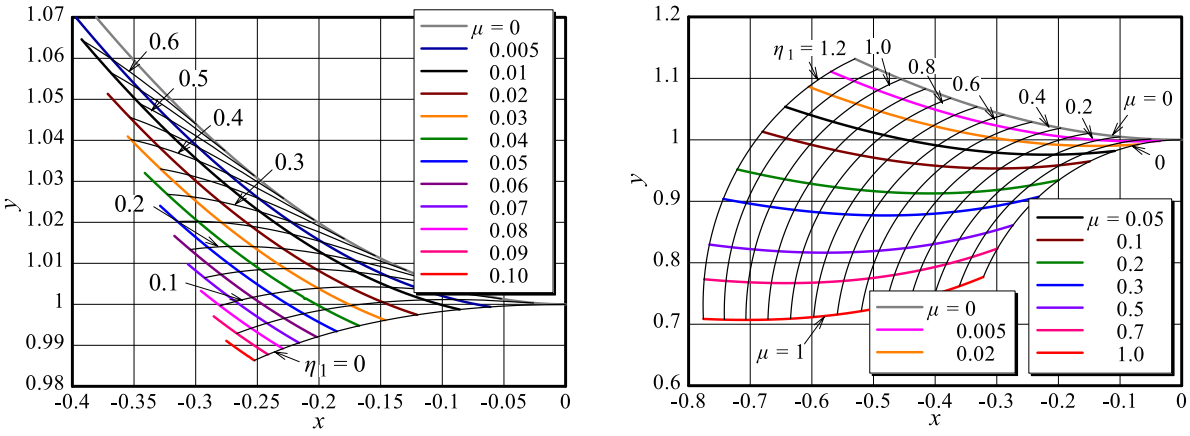

(a) System with a series-type double-mass DVA (b) System with a single-mass DVA

Fig. 4 Trajectories of the characteristic root when a hysteretically damped system takes a multiple root. In a hysteretically damped system, the region in which there is a triple root is very narrow. The gray curve (indicated by $\mu = 0$) is the trajectory of the characteristic root of the system without a DVA, and, in contrast to the viscously damped system, the higher the damping of the hysteretically damped system, the higher the natural angular frequency. The curve $\eta_1 = 0$ in (a) represents Eq. (9) and is considerably shifted to the left in comparison with that in (b).

[DOI: 10.1299/mej.20-00476]

Fig. 4(b); however, as shown in Fig. 4(a), the curve rises to the left when η_1 is large. This means that in a system with a DVA optimized by the stability criterion, the damped natural frequency can be increased by installing a larger DVA. Furthermore, this figure demonstrates that the characteristic equation takes a triple root only up to $\mu = 1/9$ for $\eta_1 = 0$ but the area in which the roots exist becomes narrower with increasing η_1.

4.5. Optimal solutions and maximized stability criterion

Figure 5(a)–(d) illustrates the optimal design conditions for the hysteretically damped series-type double-mass DVA calculated from Eqs. (13) and (14). The design parameter η_2 of the DVA is zero. In addition, Fig. 5(e) shows the stability

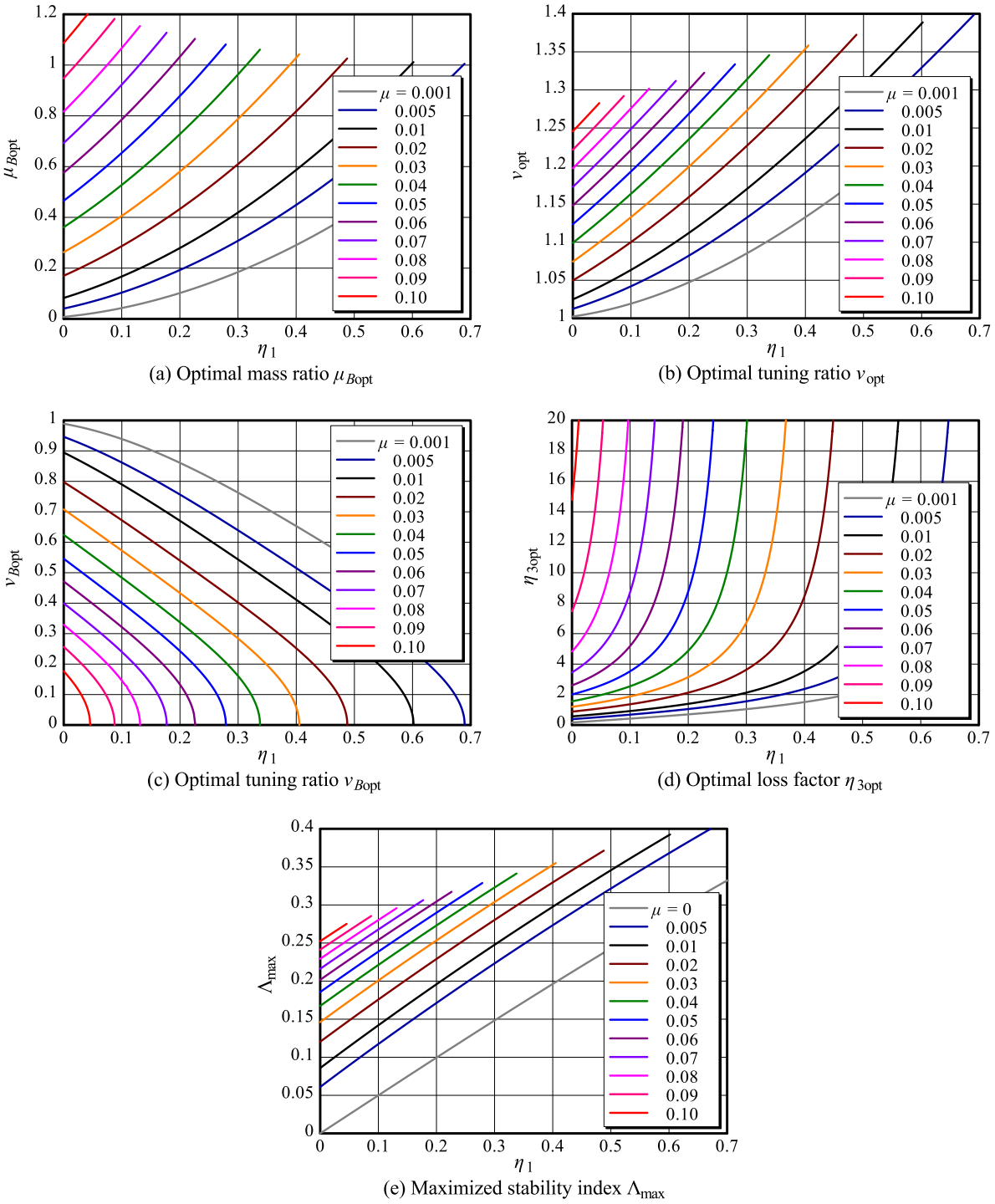

(a) Optimal mass ratio μ_{Bopt}

(b) Optimal tuning ratio v_{opt}

(c) Optimal tuning ratio v_{Bopt}

(d) Optimal loss factor η_{3opt}

(e) Maximized stability index Λ_{max}

Fig. 5 Dimensionless parameters for a hysteretically damped double-mass DVA attached to a hysteretically damped primary system optimized with the stability criterion. The optimal tuning ratio v_{Bopt} of DVA-*B* to DVA-*A* is exactly zero for a certain loss factor η_1 of the primary system. At this moment, the optimal loss factor η_{3opt} of DVA-*B* diverges to infinity. (e) indicates that the stability of the system increases with the mass of the DVA system and the loss factor of primary system.

[DOI: 10.1299/mej.20-00476]

of the vibratory system calculated from the first formula in Eq. (16) (with $\Lambda_{\max} = -x_1$). In Fig. 5, the optimal values of $\eta_1 = 0$ are consistent with those calculated from Eq. (11). As shown in Fig. 5(a)–(d), the design parameters for the DVA only monotonically increase or decrease as the loss factor η_1 of the primary system increases. In particular, the undamped natural angular frequency ratio of DVA-*B* to -*A* is zero for a certain value of η_1. At this time, the optimal value of the loss factor of DVA-*B*, $\eta_{3\mathrm{opt}}$, is infinite. Although the optimal design condition for the DVA may exist after the point where $\nu_{B\mathrm{opt}} = 0$, it is not possible to search for this method using the "condition that the characteristic equation takes a triple root" adopted in this paper. As shown in Fig. 5(e), the maximum value of the stability of the vibrating system, $\Lambda_{\max}$, increases with the mass of the DVA and the loss factor for the primary system. In particular, the large difference between the curves for $\mu = 0$ and $\mu = 0.005$ shows that even a small DVA has a great effect on the stability of the vibratory system.

4.6. Free-vibration responses of optimized vibratory system

Figure 6(a) and (b) show the free-vibration response of a vibratory system with a hysteretically damped double-mass DVA with $\mu = 0.05$ and 0.1, respectively. In the calculation of the results, including Figs. 7 and 8, it was assumed that the primary system is undamped ($\eta_1 = \zeta_1 = 0$). In addition, the initial conditions for these calculations are as follows:

$$x_1(0) = 0, \quad \dot{x}_1(0) = v_0, \quad x_2(0) = 0, \quad \dot{x}_2(0) = 0, \quad x_3(0) = 0, \quad \dot{x}_3(0) = 0. \tag{17}$$

That is, the initial velocity v_0 is applied only to the primary mass, and the initial displacement and velocity are zero for both DVA-*A* and -*B*. As shown in Fig. 6(a) and (b), the kinetic energy given to the primary mass is transferred from the primary system to DVA-*A*, and then from DVA-*A* to DVA-*B*, and the energy is gradually lost (i.e., dissipated as thermal

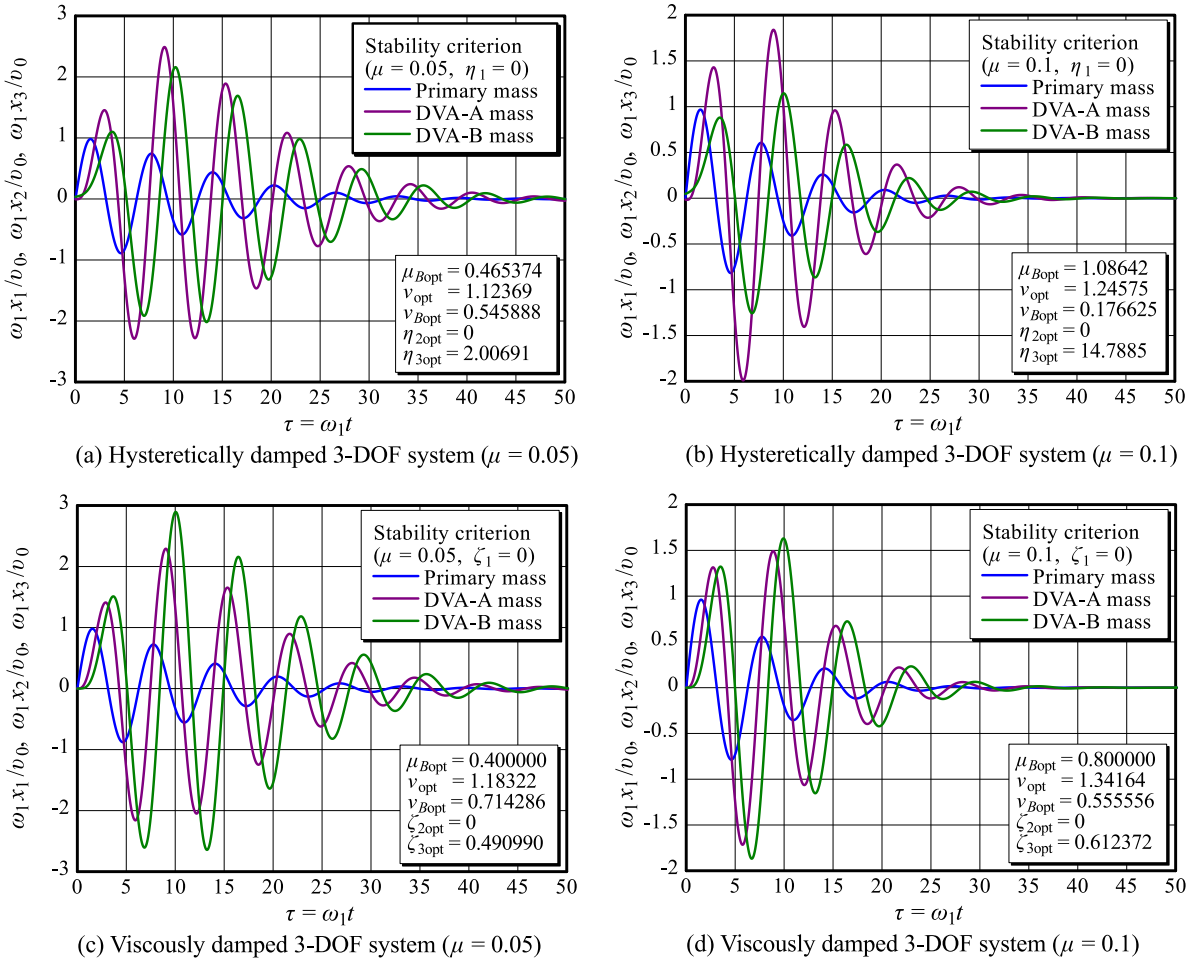

(a) Hysteretically damped 3-DOF system ($\mu = 0.05$)

(b) Hysteretically damped 3-DOF system ($\mu = 0.1$)

(c) Viscously damped 3-DOF system ($\mu = 0.05$)

(d) Viscously damped 3-DOF system ($\mu = 0.1$)

Fig. 6 Free-vibration responses of a 3-DOF vibratory system optimized by the stability criterion. The three curves show the responses of the primary system, DVA-*A*, and DVA-*B* after an initial velocity is applied to the primary system. A system with a DVA optimized by the stability criterion is characterized by the fact that the kinetic energy flows in one direction from the primary system to the DVA and does not cause back-vibration. The major difference between hysteretically ((a) and (b)) and viscously ((c) and (d)) damped systems is the relationship between the magnitude of the responses of DVA-*A* and -*B*.

[DOI: 10.1299/mej.20-00476]

energy) by the internal damping of the connecting springs. Because there is no energy backflow from DVA-*A* to the primary system, the DVAs act like a damper, and the vibrations converge monotonically with time, just like the free vibration of a damped single-degree-of-freedom (SDOF) system. Figure 6(c) and (d) shows the free-vibration response of a system with a viscously damped DVA optimized by the stability criterion. The response of this primary system is not much different from that of the hysteretically damped system, but there is a significant difference between the relationships of the magnitudes of the responses of DVA-*A* and -*B* in the hysteretically and viscously damped systems.

Figures 6–8 show the free-vibration responses calculated as the superposition of the forced-vibration response using a method developed by one of the authors (Yamada, 2020). The analytical model presented in Fig. 1(a) is based on the assumption that periodic external forces act on the system. Therefore, by decomposing the applied impulse into a Fourier series expansion and calculating the steady-state response at each frequency, the free-vibration response of the system to the impulse can be calculated by superimposing them.

For simplicity, this method is illustrated in a viscously damped SDOF system. The equation of motion is

$$m\ddot{x}_1 + c\dot{x}_1 + kx_1 = f. \tag{18}$$

Here, the excitation force f is considered to be an impulse, and its Fourier series expansion is expressed by

$$f = P_m\delta(t) = \frac{a_0}{2} + \sum_{k=1}^{\infty}(a_k \cos\omega_k t + b_k \sin\omega_k t), \quad \text{where} \quad \omega_k = \frac{k\pi}{T}, \tag{19}$$

where a_0, a_k, and b_k are the Fourier coefficients. Finding these Fourier coefficients for the applied impulse and substituting them into Eq. (18) gives

$$m\ddot{x}_1 + c\dot{x}_1 + kx_1 = \frac{P_m}{2T} + \sum_{k=1}^{\infty}\frac{P_m}{T}\cos\omega_k t. \tag{20}$$

Because this is a linear equation, the responses x_1 at different frequencies can be calculated and superimposed to obtain the free-vibration response to the applied impulse. If the free vibrations are represented by the superposition of forced vibrations, the same formula can be used to calculate the response of the system regardless of whether the system is under-damped, critically-damped or over-damped.

The following equations were used to calculate the free-vibration responses shown in Figs. 6(a) and 6(b) for the hysteretically damped 3-DOF system.

$$x_1 = \frac{P_m}{2Tk_1} + \frac{P_m}{Tk_1}\sum_{k=1}^{\infty}\frac{\text{Num1}}{\text{Den}}e^{i\omega_k t}, \quad x_2 = \frac{P_m}{2Tk_1} + \frac{P_m}{Tk_1}\sum_{k=1}^{\infty}\frac{\text{Num2}}{\text{Den}}e^{i\omega_k t}, \quad x_3 = \frac{P_m}{2Tk_1} + \frac{P_m}{Tk_1}\sum_{k=1}^{\infty}\frac{\text{Num3}}{\text{Den}}e^{i\omega_k t}, \tag{21}$$

where

$$\left.\begin{aligned}
&\text{Num1} = -(1+\mu_B)\{\lambda_k^4 - \nu^2[1+(1+i\eta_3)(1+\mu_B)\nu_B^2]\lambda_k^2 + (1+i\eta_3)\nu^4\nu_B^2\}\\
&\text{Num2} = (1+\mu_B)\nu^2[\lambda_k^2 - (1+i\eta_3)\nu^2\nu_B^2], \quad \text{Num3} = -(1+\mu_B)(1+i\eta_3)\nu^4\nu_B^2\\
&\text{Den} = (1+\mu_B)\lambda_k^6 - \{1+\mu_B+(1+i\eta_3)\,\mu_B^2\nu^2\nu_B^2 + \mu_B\nu^2[1+2(1+i\eta_3)\nu_B^2] + \nu^2[1+\mu+(1+i\eta_3)\nu_B^2]\}\lambda_k^4\\
&\qquad + (1+\mu_B)\nu^2\{1+(1+i\eta_3)\,[1+\mu_B+(1+\mu)\nu^2]\nu_B^2\}\lambda_k^2 - (1+\mu_B)(1+i\eta_3)\nu^4\nu_B^2.
\end{aligned}\right\} \tag{22}$$

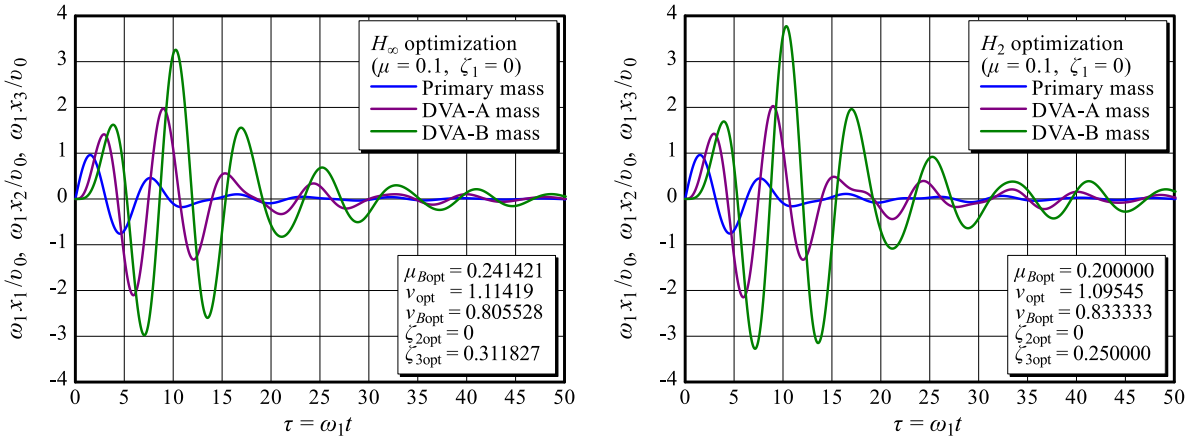

(a) H_∞ optimization of a 3-DOF system ($\mu = 0.1$) (b) H_2 optimization of a 3-DOF system ($\mu = 0.1$)

Fig. 7 Free-vibration responses of a viscously damped 3-DOF system optimized by the H_∞ and H_2 criteria. In a vibratory system with DVAs designed with these criteria, the initial vibration decay of the primary system is fast, but the slow vibration decay of the DVA causes energy backflow, that is, it introduces vibration back to the primary system. As a result, the final convergence of the vibrations is slow.

[DOI: 10.1299/mej.20-00476]

Here, the values of η_1 and η_2 are set to zero. Then, by expressing Eq. (21) in a dimensionless form, and replacing the infinity symbol by a finite value of n, we obtain

$$\frac{\omega_1}{v_0}x_1 = \frac{1}{2T\omega_1}+\frac{1}{T\omega_1}\sum_{k=1}^{n}\frac{\mathrm{Num1}}{\mathrm{Den}}e^{i\tau_k},\quad \frac{\omega_1}{v_0}x_2 = \frac{1}{2T\omega_1}+\frac{1}{T\omega_1}\sum_{k=1}^{n}\frac{\mathrm{Num2}}{\mathrm{Den}}e^{i\tau_k},\quad \frac{\omega_1}{v_0}x_3 = \frac{1}{2T\omega_1}+\frac{1}{T\omega_1}\sum_{k=1}^{n}\frac{\mathrm{Num3}}{\mathrm{Den}}e^{i\tau_k}. \quad (23)$$

The symbols $\lambda_k = \omega_k/\omega_1$ and $\tau_k = \omega_k t$ (where $\omega_k = k\pi/T$) used in Eqs. (22) and (23) denote the discretized dimensionless frequency and time, respectively. Finally, a physically meaningful solution can be obtained by extracting the real part of Eq. (23). Figures 6(a) and 6(b) show the results for the dimensionless quantities $T\omega_1 = 200$ and $n = 10,000$.

Figure 7 shows the free-vibration responses of a viscously damped 3-DOF system designed by optimization criteria other than the stability criterion: the H_∞ and H_2 criteria. Figure 6 indicates that the free-vibration responses of the primary system do not differ significantly between the hysteretically and viscously damped systems. Therefore, because the H_∞ and H_2 optimal solutions for the hysteretically damped 3-DOF system are not currently available, we compare the free-vibration responses for viscously damped systems designed by these optimization criteria with each other. A comparison of Figs. 7 and 6(d) demonstrates that the final convergence of the vibrations is considerably faster if the DVA is designed by the stability criterion. In addition, expressing the free-vibration response by superimposing forced vibrations is especially convenient when the characteristic equation take a multiple root.

In Figs. 7, 6(c) and 6(d), the optimal DVA parameters are calculated using the following equations (Asami, 2019). For the H_∞ optimization criterion:

$$\mu_{B\mathrm{opt}} = \left(1+\sqrt{2}\right)\mu,\quad \nu_{\mathrm{opt}} = \sqrt{1+\left(1+\sqrt{2}\right)\mu},\quad \nu_{B\mathrm{opt}} = \frac{1}{1+\left(1+\sqrt{2}\right)\mu},\quad \zeta_{2\mathrm{opt}} = 0,\quad \zeta_{3\mathrm{opt}} = \sqrt{\frac{1}{2}\frac{\left(1+\sqrt{2}\right)\mu}{1+\left(1+\sqrt{2}\right)\mu}}. \quad (24)$$

For the H_2 optimization criterion:

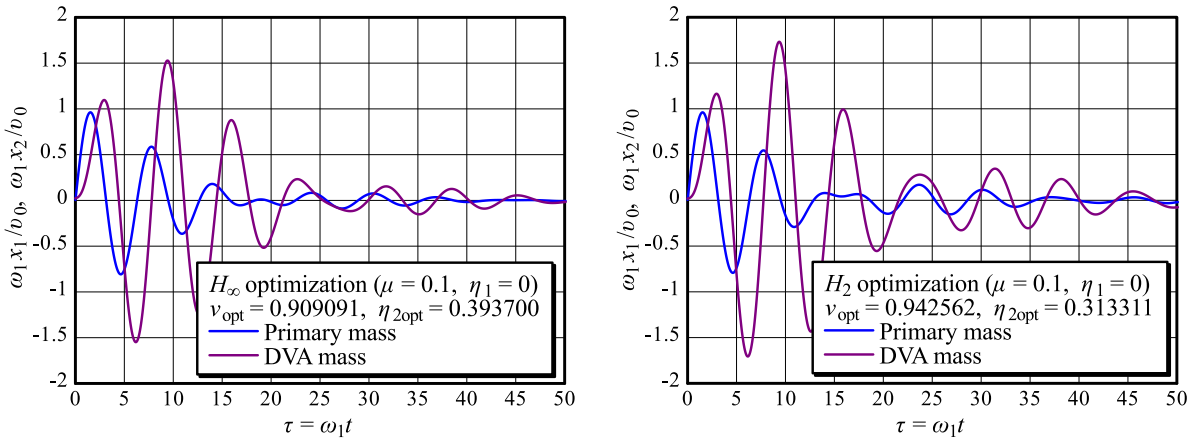

(a) H_∞ optimization of a 2-DOF system ($\mu = 0.1$)

(b) H_2 optimization of a 2-DOF system ($\mu = 0.1$)

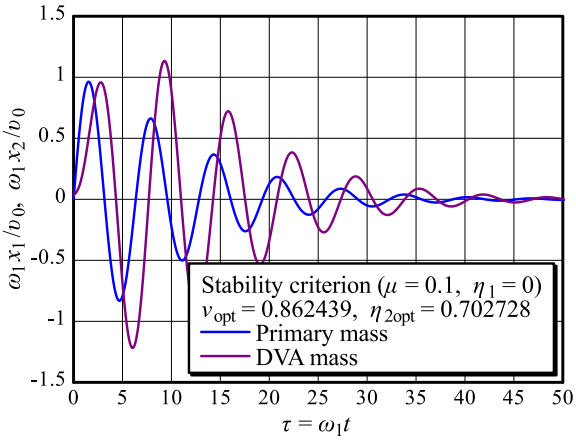

(c) Stability criterion of a 2-DOF system ($\mu = 0.1$)

Fig. 8 Free-vibration responses of a hysteretically damped 2-DOF system optimized by the H_∞, H_2 and stability criteria. The vibrations converge more slowly than in Fig. 6, which represents the free-vibration response of the system with a double-mass DVA installed. When the DVA is optimally designed with the stability criterion, the initial decay of the primary system is gradual, but the vibration converges most quickly in the end because there is no back-vibration.

[DOI: 10.1299/mej.20-00476]

$$\mu_{B\mathrm{opt}} = 2\mu, \quad \nu_{\mathrm{opt}} = \sqrt{1+2\mu}, \quad \nu_{B\mathrm{opt}} = \frac{1}{1+2\mu}, \quad \zeta_{2\mathrm{opt}} = 0, \quad \zeta_{3\mathrm{opt}} = \frac{1}{2}\sqrt{\frac{3\mu}{1+2\mu}}. \tag{25}$$

For the stability maximization criterion:

$$\mu_{B\mathrm{opt}} = 8\mu, \quad \nu_{\mathrm{opt}} = \sqrt{1+8\mu}, \quad \nu_{B\mathrm{opt}} = \frac{1}{1+8\mu}, \quad \zeta_{2\mathrm{opt}} = 0, \quad \zeta_{3\mathrm{opt}} = \frac{3}{2}\sqrt{\frac{3\mu}{1+8\mu}}. \tag{26}$$

Figure 8 shows the free-vibration responses of systems with hysteretically damped single-mass DVAs optimally designed by the three different optimization criteria. As shown in this figure, when the DVA is designed by the stability criterion, the initial vibration decay of is slow. However, the vibration convergence was most rapid at the end because of the absence of energy backflow from the DVA to the primary system. A comparison of Figs. 8(c) and 6(b) reveals that the vibration convergence is even faster when two DVAs are used.

4.7. Steady-state responses of the optimized vibratory system

Figure 9 shows the steady-state responses of the primary system for a hysteretically damped 3-DOF (primary system + series-type double-mass DVA) and 2-DOF (primary system + single-mass DVA) systems with an applied periodic external force. Figure 9(a) and (b) shows the calculation results for the 3-DOF system with different values of μ, only up to $\eta_1 = 0.25$ and $\eta_1 = 0.04$, respectively. When the DVA is designed based on the stability criterion, the damping magnitude (loss factor) of the DVA is designed to be quite large, so that the steady-state response of the multi-degree-of-freedom system will necessarily have a single resonant point, as if it is a SDOF system. A comparison of the heights of the resonant points in the 3- and 2-DOF systems, reveals that the resonant point of the 3-DOF system is lower than that of the 2-DOF system for the same mass ratio μ and primary system loss factor η_1.

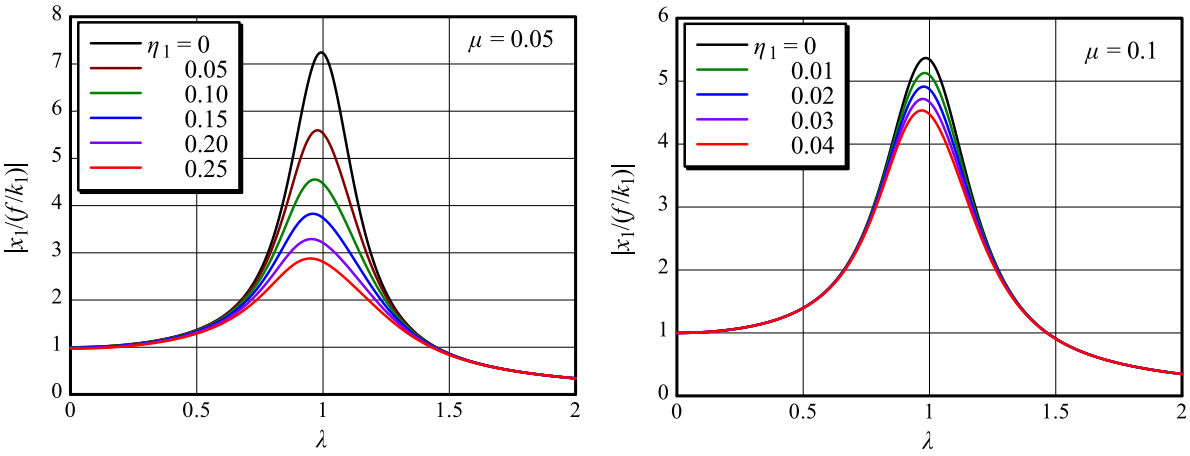

(a) Steady-state response of a 3-DOF system ($\mu = 0.05$)

(b) Steady-state response of a 3-DOF system ($\mu = 0.1$)

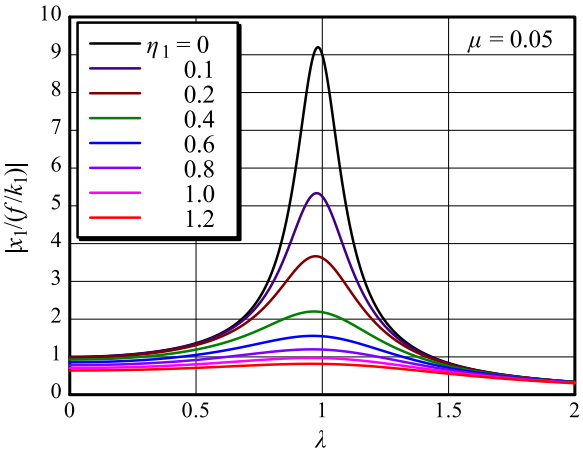

(c) Steady-state response of a 2-DOF system ($\mu = 0.05$)

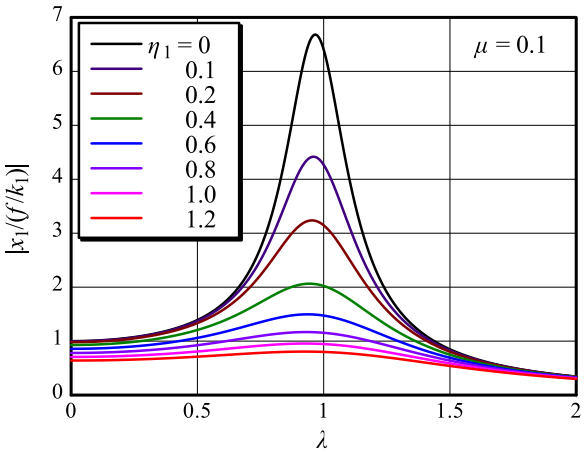

(d) Steady-state response of a 2-DOF system ($\mu = 0.1$)

Fig. 9 Steady-state responses of a hysteretically damped 3- and 2-DOF systems optimized by the stability criterion. Because the DVA designed with the stability criterion is given a fairly large damping, only one resonant point appears in the optimized response. These plots show that the stability increase also contributes to reducing the height of the resonant point in the steady-state response. The range of loss coefficients for the primary system is narrower in (a) and (b) because the region in which the characteristic equations can take a triple root is quite narrow.

[DOI: 10.1299/mej.20-00476]

5. Conclusion

This paper is a continuation of our previously published paper (Asami et al., 2020). In this previous paper, we discussed the optimal design method for a hysteretically damped single-mass DVA, where the DVA was designed using three optimization criteria: H_∞ optimization, H_2 optimization and stability maximization. In this study, two DVAs were connected in series to improve their performance, and were optimized by the stability maximization criterion. The results of this study are summarized as follows:

(1) If there is no damping in the primary system, the four design parameters of the DVA (five if η_2 is included) can be optimized by a very simple formula. In contrast, if there is damping in the primary system, the optimal solution can be calculated numerically using Eqs. (13)–(15).

(2) The stability of the vibratory system was approximately 1.7 times greater than that with a single-mass DVA when the optimized series-type double-mass DVA was installed.

(3) As the stability of the system increases, the free-vibration response converges faster and the height of the resonant point in the steady-state response decreases.

Acknowledgment

The general-purpose math processing software *Mathematica* Ver.12.0 was used for the execution of this research. This work was supported by a Grant-in-Aid (19K04276) for Scientific Research from the Ministry of Education, Culture, Sports, Science and Technology of Japan. The authors would like to express their gratitude for this support.

References

Asami, T., Optimal Design of Double-Mass Dynamic Vibration Absorbers Arranged in Series or in Parallel, ASME J. Vib. Acoust., Vol.139, No.1 (2017), DOI: 10.1115/1.4034776.

Asami, T., Mizukawa, Y., and Ise, T., Optimal Design of Double-Mass Dynamic Vibration Absorbers Minimizing the Mobility Transfer Function, ASME J. Vib. Acoust., Vol.140, No.6 (2018), DOI: 10.1115/1.4040229.

Asami, T., Exact Algebraic Solution of an Optimal Double-Mass Dynamic Vibration Absorbers Attached to a Damped Primary System, ASME J. Vib. Acoust., Vol.141, No.5 (2019), DOI: 10.1115/1.4043815.

Asami, T., and Yamada, K., Numerical Solutions for Double-Mass Dynamic Vibration Absorbers Attached to a Damped Primary System, Bull. of the JSME Mechanical Engineering Journal, Vol.7, No.2 (2020), DOI:10.1299/mej.19-00051.

Asami, T., Mizukawa, Y., and Yamada, K., Optimal Design of a Hystererically Damped Dynamic Vibration Absorber, Bull. of the JSME Mechanical Engineering Journal, Vol.7, No.2 (2020), DOI:10.1299/mej.19-00482.

Crandall, S. H., and Mark, W. D., Random Vibration in Mechanical Systems, (1963), Academic Press, p.71.

Iwanami, K., and Seto, K., An Optimum Design Method for the Dual Dynamic Damper and Its E ffectiveness, Bull. of JSME, Vol.27, No.231 (1984), pp.1965-1973, DOI: 10.1299/jsme1958.27.1965.

Nishihara, O., and Matsuhisa, H., Design and Tuning of Vibration Control Devices via Stability Criterion, Dynamics and Design Conference '97, No.97-10-1 (1997), pp.165-168, (in Japanese).

Ormondroyd, J., and Den Hartog, J. P., The Theory of the Dynamic Vibration Absorber, ASME Journal of Applied Mechanics, Vol.50, No.7 (1928), pp.9-22.

Shibata, K., Misaji, K., and Kato, H., Vibration Characteristics of Rubber (Nonlinear Vibration Characteristics Depending on Frequency and Amplitude of Displacement), Transactions of the JSME, Ser. C, Vol.59, No.564 (1993), pp.2408-2414, (in Japanese), DOI: 10.1299/kikaic.59.2408.

Yamada, K., Free Vibration Analysis of Vibration System with Hysteretic Damping, Dynamics and Design Conference 2020, No.20-11 (2020), p.257(12 pages), (in Japanese).

Yasuda, M., and Pan, G., Optimization of Two-Series-Mass Dynamic Vibration Absorber and Its Vibration Control Performance, Transactions of the JSME, Ser. C, Vol.69, No.688 (2003), pp.3175-3182, (in Japanese), DOI: 10.1299/kikaic.69.3175.

Watts, P., On a Method of Reducing the Rolling of Ship at Sea, Transactions of the Institution of Naval Architects, Vol.24 (1883), pp.165-190.

[DOI: 10.1299/mej.20-00476]